Journal of Hazardous Materials Letters 3 (2022) 100072

Contents lists available at ScienceDirect

Journal of Hazardous Materials Letters

journal homepage: www.sciencedirect.com/journal/journal-of-hazardous-materials-letters

Hydrogen-polarized vacuum ultraviolet photolysis system for enhanced destruction of perfluoroalkyl substances

Gongde Chen [a,*], Sitao Liu [a], Qingyang Shi [b], Jay Gan [b], Bosen Jin [a], Yujie Men [a], Haizhou Liu [a,*]

[a] Department of Chemical and Environmental Engineering, University of California, Riverside, CA 92521, USA
[b] Department of Environmental Sciences, University of California, Riverside, CA 92521, USA

ARTICLE INFO

Keywords:
Vacuum UV
PFAS
Destruction
Water ionization
Defluorination

ABSTRACT

Reductive water treatment using hydrated electrons (e^-_{aq}) is a promising technology to destruct perfluoroalkyl substances; however, it faces challenges of slow reaction kinetics, undesirable chemical addition, and high energy consumption. Herein, we developed a hydrogen (H_2)-polarized water photolysis system using vacuum UV (VUV) light at 185 nm for reductive destruction of perfluorooctanoic acid (PFOA) and perfluorooctanesulfonic acid (PFOS). The 185-nm photons directly photolyzed H_2O and OH^- into HO·, H·, and e^-_{aq}. H_2 elevated the *quasi* steady-state concentration of e^-_{aq} 18 times in untuned VUV systems through eliminating the scavenging effect of dissolved oxygen and converting hydroxyl radicals (HO·/$O^{\cdot-}$) into e^-_{aq}. The polarization effect of H_2 increased the degradation of PFOA from 10 % to 95 % and the defluorination from 17 % to 94 % and led to 87 % of defluorination for PFOS. The pH impacted VUV photon adsorption between H_2O and OH^- and shifted the equilibrium between H· and e^-_{aq}, which led to an optimal pH of 10.3 for PFOA destruction. The presence of chloride and sulfate enhanced the production of e^-_{aq} and promoted PFOA destruction. H_2-polarized VUV water photolysis systems produced high levels of e^-_{aq} from clean water constituents and significantly reduced energy consumption for PFAS treatment under mild alkaline conditions.

1. Introduction

The wide application and improper disposal of poly- and perfluoroalkyl substances (PFAS) lead to their ubiquitous occurrence in terrestrial, aquatic and atmospheric environments, which poses a great threat to public health (United State Environmental Protection Agency: Our Current Understanding of the Human Health and Environmental Risks of PFAS; Hu et al., 2016; Glüge et al., 2020). The U.S. EPA recently released updated health advisories for four types of PFAS (United State Environmental Protection Agency: Drinking Water Health Advisories for PFAS Fact Sheet for Communities). Physical treatment processes, including activated carbon adsorption (Park et al., 2020; McCleaf et al., 2017; Xiao et al., 2017), ion exchange, (Liu and Sun, 2021; Boyer et al., 2021; Fang et al., 2021) and membrane separation (Mastropietro et al., 2021; Lee et al., 2021; Xiong et al., 2021), only physically transfer PFAS from the contaminated water to a second media (either as spent media or concentrate). Conventional chemical oxidants (*e.g.*, chlorine and permanganate) and reductants (*e.g.*, ferrous ion and zero-valent iron) are ineffective in breaking highly stable C—F bonds under ambient environmental conditions (Dombrowski et al., 2018; Vecitis et al., 2009,) Microbial PFAS degradation is normally slow (Zhang et al., 2022; Wackett, 2022; Huang and Jaffé, 2019; Yu et al., 2022). Thermal incineration is energy intensive and likely induces a secondary atmospheric PFAS pollution due to incomplete combustion (Wang et al., 2022a, 2022b; Stoiber et al., 2020).

Reductive defluorination using hydrated electrons (e^-_{aq}) is an effective approach to degrade PFAS compounds (Fennell et al., 2022; Cui et al., 2020; Chen et al., 2021; Bentel et al., 2020; Kugler et al., 2021). The negative reduction potential of e^-_{aq} ($E^o = -2.9$ V) leads to a low free energy activation barrier for C-F bond cleavage (Biswas et al., 2022; Yamijala et al., 2020). e^-_{aq} is traditionally produced by UVC ($\lambda = 254$ nm) photolysis of ionizable chemicals (*e.g.*, sulfite and indole compounds) (Fennell et al., 2022; Cui et al., 2020; Chen et al., 2021; Bentel et al., 2020; Liu et al., 2022; Park et al., 2009). However, this process suffers from a low quantum yield of e^-_{aq} ($\Phi = 0.11$–0.29), a high chemical dosage (mM levels), and the formation of by-products that requires additional purification (Fennell et al., 2022; Cui et al., 2020; Liu

* Corresponding authors.
E-mail addresses: gchen016@ucr.edu (G. Chen), haizhou@engr.ucr.edu (H. Liu).

https://doi.org/10.1016/j.hazl.2022.100072
Received 2 September 2022; Received in revised form 17 October 2022; Accepted 7 November 2022
Available online 8 November 2022

et al., 2022; Yu et al., 2018). Recently, e_{aq}^--based PFAS treatment using water ionization systems has attracted much attention (Gonzalez et al., 2004; Zoschke et al., 2014; Locke et al., 2006; Attri et al., 2018; Ponomarev and Ershov, 2020). In these systems, an energetic medium, including vacuum UV (VUV) light (λ = 100–200 nm), non-thermal plasma, gamma rays, and electron beam, directly dissociates water molecules into a variety of reactive species (*e.g.*, e_{aq}^-, H· and HO·). VUV light is one of the most convenient water ionization media, because it can be readily generated from commonly used mercury lamps and conveniently operated (Gonzalez et al., 2004; Zoschke et al., 2014). However, conventional VUV systems exhibit slow PFAS degradation, inadequate defluorination, and a high energy consumption (Jin and Zhang, 2015; Jing et al., 2007; Wang and Zhang, 2014; Chen and Zhang, 2006), due to low quantum yield of e_{aq}^- (Φ = 0.045), high e_{aq}^--scavenging effect from common water constituents (*e.g.*, dissolved oxygen, nitrate, bicarbonate, and dissolved organic carbon), and incapable utilization of the major reactive species (*e.g.*, HO· and H·) in VUV systems (Fennell et al., 2022; Zoschke et al., 2014; Wang and Zhang, 2014).

To transform VUV systems into highly efficient platforms for PFAS destruction, it is essential to minimize the scavenging effects and tune the speciation of reactive species to enhance the production of e_{aq}^-. Prior studies on transient reactive species in pulse radiolysis systems showed that H_2 could convert HO·/$O^{\cdot-}$ radicals into e_{aq}^- under alkaline conditions (Wardman, 1978; Hickel and Sehested, 1991). Given the unique role of H_2 in deoxygenation, radical conversion and its sustainable nature in clean final product (*i.e.*, water), harnessing H_2 in VUV systems can create e_{aq}^--dominated highly reducing environments for efficient and sustainable treatment of PFAS. In addition, VUV light can beneficially photolyze common water constituents (*e.g.*, chloride and sulfate) to enhance the production of e_{aq}^- (Duca et al., 2017; Barki et al., 2021; Jortner et al., 1964; Furatian and Mohseni, 2018a, 2018b). Accordingly, we developed a highly polarized water photolysis system utilizing H_2 to boost the treatment and energy efficiency. VUV water photolysis was selected as a model water ionization system to produce a representative mixture of primary reactive species. We investigated the degradation and defluorination of PFOA and PFOS in a H_2-polarized VUV system, quantified the effects of solution pH and coexisting constituents on the speciation and yield of reactive species, and monitored the transformation products of PFOA and PFOS.

2. Materials and methods

Information on all chemicals and equipment used is provided in Text S1 in the Supporting information (SI). Photochemical experiments were performed in a cylindrical borosilicate glass reactor. Four low-pressure mercury lamps (52 W) housed in high-transmittance synthetic quartz sleeves served as light sources and were immersed into the solution (Text S1 and Scheme S1). The lamps have major output at 254 nm accompanied with emission at 185 nm (irradiation intensity: $I_{185\,nm}$ = 8 % $I_{254\,nm}$) (Zoschke et al., 2014; Masschelein and Rice, 2016). N_2 gas (99.97 %) continuously purged lamp-housing quartz sleeves to minimize the attenuation of 185-nm VUV light by air. Typically, a 500-mL solution containing 2.5–25 μM of PFOA or PFOS was treated in the photochemical reactor. The solution was pre-saturated with H_2 (99.99 %) for 30 min and was continuously sparged with H_2 throughout the reaction. Control experiments were performed in solutions saturated with N_2, N_2O or air, or irradiated by UVC mercury lamps (λ = 254 nm) with titanium-doped quartz envelopes that blocked the 185-nm VUV light. To test the effect of pH on PFOA treatment, the initial solution pH varied between 7.0 and 12.0 using NaOH. To investigate the effect of coexisting constituents, experiments were conducted in H_2-saturated VUV systems in the presence of 5 mM chloride, 5 mM sulfate, 5 mM carbonate, or 5.4 mg-C/L Suwannee River humic acid. These concentrations were chosen to represent high levels measured in groundwater. To assess the treatment efficiency for PFAS in a real drinking water matrix, experiments were conducted using tap water from Riverside, CA (Table S1) with spiked PFOA or PFOS. All experiments were conducted at 22 °C.

The concentrations of fluoride ions were measured by fluoride ion selective electrode with accuracy verified by ion chromatography (Fig. S1). The defluorination extent was calculated as the molar concentration ratio of the measured fluoride ions at a given reaction time to total fluorine in PFAS compounds initially present in the solution. PFAS parent compounds and their transformation products were measured by an ultra-high-performance liquid chromatography system equipped with a high-resolution mass spectrometer (UPLC–HRMS). Additional information on experimental setup and analytical procedures is provided in Text S1 and Table S2 of the SI.

3. Results and discussion

3.1. Enhanced destruction of PFAS in the H_2-polarized VUV systems

The untuned VUV system (*i.e.*, VUV/air in which solution was air-saturated; Figs. 1A and 1B) was inefficient in destruction of PFOA, only exhibiting 23 % defluorination and 58 % degradation after 180 min of treatment. In contrast, polarizing VUV systems with H_2 gas substantially increased defluorination to 94 % and degradation to 97 %. The degradation and defluorination of PFOA followed a *pseudo* first-order kinetics (Fig. S2). The observed *pseudo* first-order rate constants (k_{obs}) in the H_2-polarized VUV system were 18 times (PFOA degradation: 0.12 *vs.* 0.0067 min^{-1}) and 23 times (PFOA defluorination: 0.034 *vs.* 0.0015 min^{-1}) higher than those in VUV/air. Similarly, PFOS underwent a fast degradation (0.05 min^{-1}) and deep defluorination (87 %) in the H_2-polarized VUV system (Fig. S3A). Filtering out VUV light completely ceased the degradation and defluorination of PFOA (*i.e.*, UVC/H_2 in which only 254-nm UVC light was dosed into solution; Figs. 1A and 1B), which confirmed that the 185-nm VUV light, rather than the UVC light, initialized aqueous reactions.

The 185-nm VUV photons directly photolyze H_2O and OH^- into HO·, H·, and e_{aq}^- (Reactions (1)–(3)) with an equilibrium between HO· and $O^{\cdot-}$ (Reaction (4)): (Gonzalez et al., 2004; Zoschke et al., 2014; Lyu et al., 2015; Boyle et al., 1969; Dainton and Fowles, 1965)

$$OH^- \xrightarrow{hv} HO\cdot + e_{aq}^- \quad \varepsilon_{OH^-,\,185nm} = 3600 M^{-1}cm^{-1} \Phi_{OH^-,185nm} = 0.11 \tag{1}$$

$$H_2O \xrightarrow{hv} H\cdot + HO\cdot \varepsilon_{H_2O,185\,nm} = 0.032\ M^{-1}cm^{-1} \Phi_{H_2O,185\,nm} = 0.33 \tag{2}$$

$$H_2O \xrightarrow{hv} H^+ + HO\cdot + e_{aq}^- \ \varepsilon_{H_2O,\,185\,nm} = 0.032\ M^{-1}\ cm^{-1} \Phi_{H_2O,\,185\,nm} = 0.045 \tag{3}$$

$$HO^{\cdot} \leftrightharpoons O^{\cdot-} + H^+ \ pK = 11.9 \tag{4}$$

Light partition calculations (Text S2 and Tables S3–S4) showed that 96 % of VUV light was absorbed by OH^- at pH 12, suggesting that hydroxyl radicals (HO·/$O^{\cdot-}$, pK = 11.9, Reaction (4)) (Poskrebyshev et al., 2002) and e_{aq}^- were the major reactive species in the VUV systems at pH 12 (Reaction (1)).

Polarizing the VUV system with H_2 has multi-fold promotive effects in creating a highly polarized reducing environment. First, H_2 converted HO· into H· (Reaction (5)) that was quickly converted into e_{aq}^- at pH 12 (H·/e_{aq}^-, pK = 9.7, Reaction (6)), and H_2 also directly converted the deprotonated hydroxyl radical (*i.e.*, $O^{\cdot-}$) into e_{aq}^- (Reaction (7)) (Hickel and Sehested, 1991; Bunn et al., 1959; Han and Bartels, 1989; Walker, 1967):

$$HO^{\bullet} + H_2 \rightarrow H\cdot + H_2O \quad k_5 = 6.0 \times 10^7 \quad M^{-1}s^{-1} \tag{5}$$

$$H\cdot + OH^- \leftrightharpoons e_{aq}^- + H_2O \quad k_6 = 2.3 \times 10^7 \quad M^{-1}s^{-1}; \quad k_{-6} = 16\ M^{-1}s^{-1} \tag{6}$$

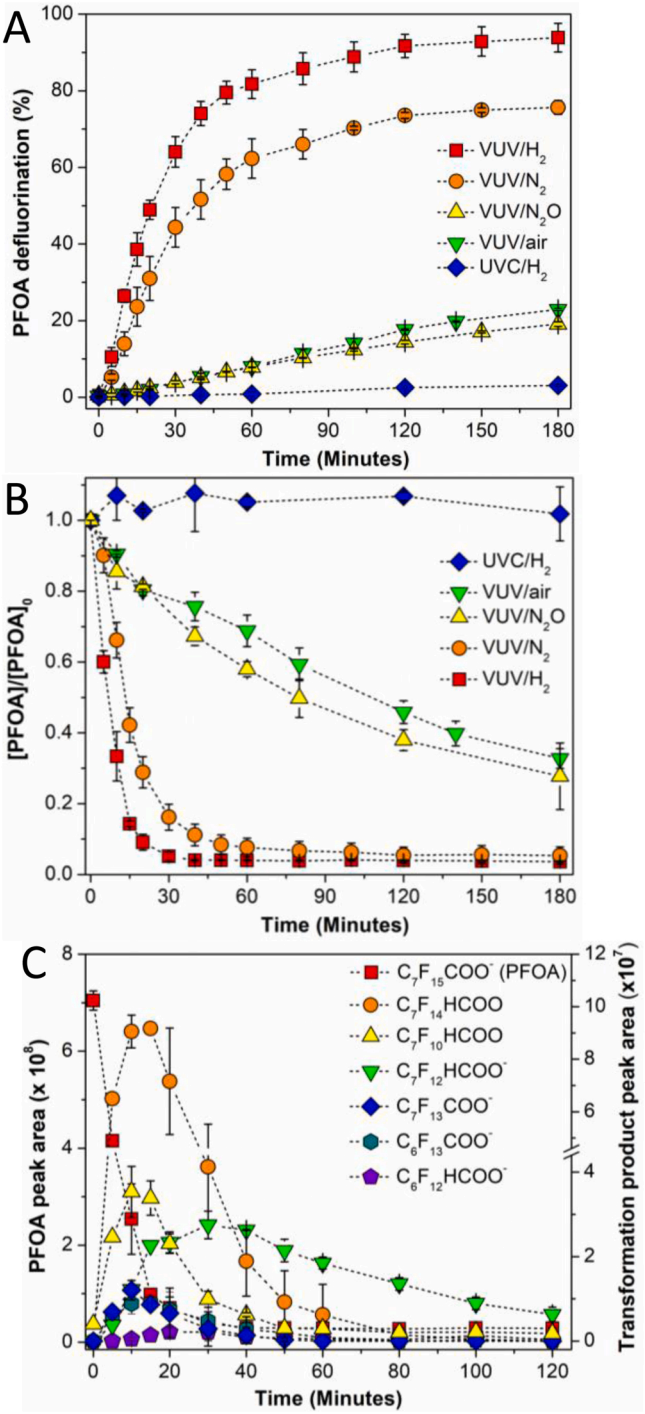

Fig. 1. Destruction of PFOA under the irradiation of VUV light (λ = 185 nm) and UVC light (λ = 254 nm). (A) Defluorination of PFOA; (B) Degradation of PFOA; (C) Evolution of transformation products. [PFOA] = 25 μM and pH = 12. Error bars represent the differences between duplicate experiments and data points represent the average.

$$O^{\bullet-} + H_2 \rightarrow e^-_{aq} + H_2O \quad k_7 = 1.1 \times 10^8 \quad M^{-1}s^{-1} \tag{7}$$

Second, H_2 deoxygenated- the solution and eliminated- the scavenging effect of dissolved oxygen on e^-_{aq} (Gordon et al., 1963):

$$e^-_{aq} + O_2 \rightarrow O_2^{\bullet-} \quad k_8 = 1.9 \times 10^{10} \quad M^{-1}s^{-1} \tag{8}$$

Branching ratio calculations (Text S3) showed that more than 99 % of e^-_{aq} was quenched by dissolved oxygen in the air-saturated VUV systems, because both the concentration of dissolved oxygen and its bimolecular rate constant with e^-_{aq} were one order of magnitude higher than those of PFOA. In contrast, when the solution was sparged with non-reactive N_2 gas, the scavenging effect of dissolved oxygen was eliminated, and the defluorination of PFOA increased from 23 % to 76 % (Fig. 1A), suggesting that deoxygenation effect of H_2 contributed to a 53 % increase in defluorination in VUV systems (*i.e.*, elimination of Reaction (8)). Replacing N_2 with H_2 further increased the defluorination from 76 % to 94 % (Fig. 1A), which was contributed by the additional production of e^-_{aq} from the reaction between H_2 and HO·/O·⁻ (Reactions (5)–(7)). Calculations (Text S4) showed that $[e^-_{aq}]_{ss}$ increased 18 times from 8.0×10^{-14} to 1.4×10^{-12} M when the air-saturated VUV system was polarized by H_2. The essential role of e^-_{aq} in destructing PFOA was further confirmed by a standard e^-_{aq}-quenching technique using N_2O gas (Buxton et al., 1988). Polarizing VUV systems with N_2O significantly slowed the destruction of PFOA (k_{obs}: 15-time decrease for PFOA degradation; 25-time decrease for PFOA defluorination), which led to a significant drop in defluorination from 90 % to 14 % (Fig. S2, Fig. 1A, and Text S3). The observed destruction of PFOA in the e^-_{aq}-quenching VUV systems (*i.e.*, VUV/N_2O) was likely due to VUV photolysis of PFOA. Collectively, the tuning effect of H_2 in deoxygenation and selective radical conversion boosted the production of e^-_{aq} and created a highly polarized reducing environment for the destruction of PFOA.

Nontarget analyses and suspect screening of UPLC-HRMS data identified six partially defluorinated/short-chain intermediates from PFOA in the H_2-polarized VUV systems (Fig. 1C). These intermediates were degraded by the end of the reaction period. In comparison to the UVC/sulfite system, three new unique intermediates with one or two alkene moieties (*i.e.*, C═C) in fluoroalkyl chain were identified: $C_7F_{13}COO^-$, $C_7F_{12}HCOO^-$, and $C_7F_{10}HCOO^-$. $C_7F_{13}COO^-$ was predicted by molecular dynamics simulations of hydrated PFOA with excess electrons and was also detected from PFOA degradation in Gamma radiation system (Yamijala et al., 2020; Patch et al., 2022). In addition, H/F exchange intermediate $C_7F_{14}HCOO^-$, chain-shortening intermediate $C_6F_{13}COO^-$ and its H/F exchange product $C_6F_{12}HCOO^-$ were also observed (Fig. 1C and Scheme S2). These three intermediates were detected in the UVC/sulfite system (Bentel et al., 2020, 2019). PFOS degradation in the H_2-polarized VUV systems generated two alkene intermediates ($C_8F_{15}SO_3^-$ and $C_8F_{14}HSO_3^-$), one OH/F exchange intermediate ($C_8F_{16}OHSO_3^-$), and one H/F exchange intermediate ($C_8F_{16}HSO_3^-$) (Fig. S3B). These intermediates were previously reported in Gamma radiation and UV sulfite systems (Bentel et al., 2020; Patch et al., 2022). The alkene intermediates from PFOA and PFOS were likely formed through H/F exchange followed by HF elimination or direct elimination of 2F from two adjacent carbons (Scheme S2) (Patch et al., 2022; Sun et al., 2021). Their formation in H_2-polarized VUV systems was likely due to the enhanced production of e^-_{aq} facilitating simultaneous dissociation of multiple C—F bonds in PFAS. The alkene moieties in PFAS structures reduced the dissociation energy of C—F bonds and enhanced the degradation and deep defluorination of PFOA and PFOS (Yamijala et al., 2020; Liu et al., 2018).

3.2. *Effect of solution pH*

Fast and complete degradation of PFOA was observed across a wide pH range in the H_2-polarized VUV systems (Fig. 2). Mild alkaline conditions accelerated the destruction process (Fig. 2). Specifically, increasing pH from 7.0 to 10.3 speeded up the defluorination rate 6 times, with the defluorination elevating from 42 % to 93 % after 100-min treatment (Fig. 2A and Fig. S4). A further increase in pH beyond 10.3 slowed the defluorination process 1.6 times. The degradation kinetics of PFOA followed the same trend as the defluorination rate constants, with the k_{obs} value (0.52 min^{-1}) peaking at pH 10.3 and decreasing by a factor of ~ 5 at a lower or higher pH (Figs. 2B and S4). The experimental results (Figs. 2 and S4) showed that the most reactive

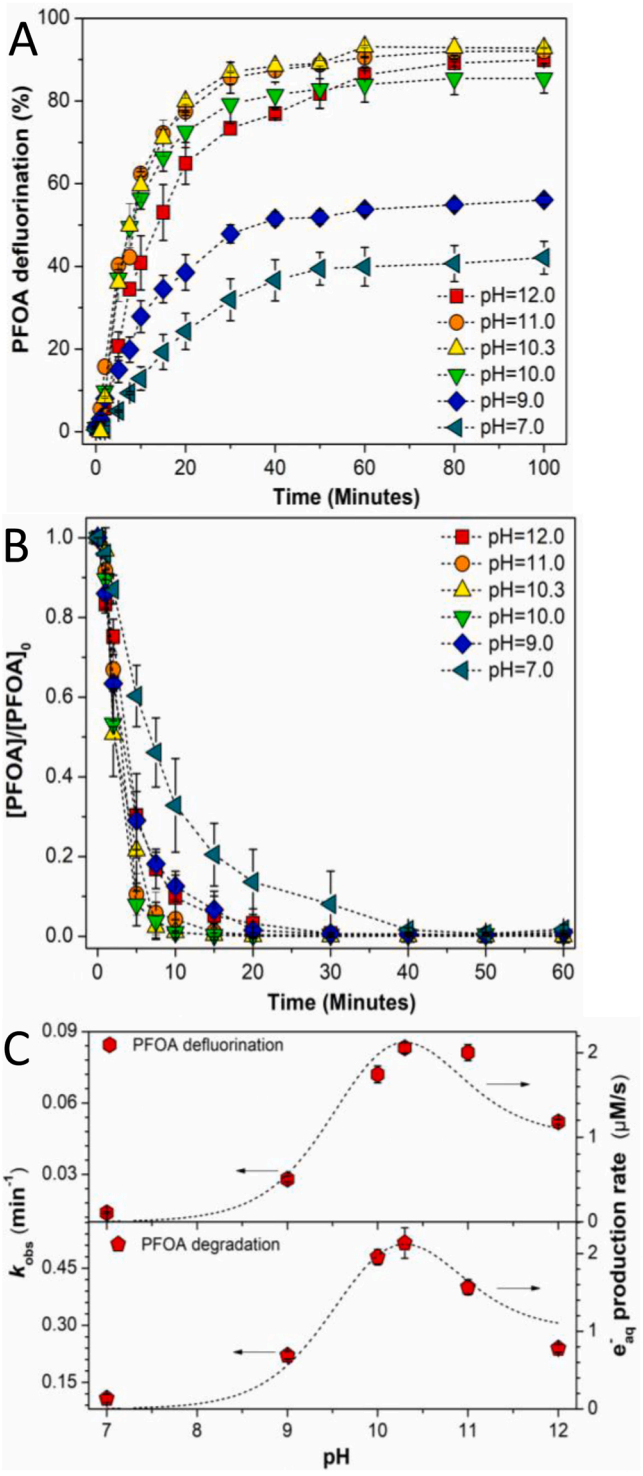

Fig. 2. Impact of initial pH on the destruction of PFOA in H_2-polarized VUV systems. (A) Defluorination of PFOA; (B) Degradation of PFOA; (C) Observed defluorination and degradation and rate constants k_{obs} (makers) and production rates of hydrated electrons (dash lines). [PFOA] = 2.5 μM. Error bars represent the differences between duplicate experiments and data points represent the average.

pH for PFOA treatment in the H_2-polarized VUV system was between 10 and 11.

The impact of pH on the defluorination and degradation rate constants of PFOA was well correlated with the production rate of e^-_{aq} (Fig. 2C). Calculations (Text S2) based on VUV volume-normalized photon irradiance to the solution in the reactor, quantum yield, and speciation of reactive species (Tables S3–S4, Text S5, and Fig. S5) showed that the production rate of e^-_{aq} increased more than two orders of magnitude from pH 7.0 to 10.3 and declined at a higher pH (Fig. 2C). The accelerated destruction of PFOA from pH 7.0 to 10.3 was due to the conversion of H· to e^-_{aq} (H·/e^-_{aq}: pK = 9.7, Reaction (6)) (Walker, 1967). As pH was above 10.3, the major species absorbing VUV photons shifted from H_2O to OH^-. Because OH^- photolysis generated much less e^-_{aq} than H_2O photolysis (Reaction (1) *vs.* Reactions (2)–(3)), the production of e^-_{aq} was reduced, which slowed the defluorination and degradation of PFOA at pH above 10.3.

3.3. *Effect of major water chemical constituents*

The presence of chloride and sulfate promoted the deep defluorination of PFOA in H_2-polarized VUV systems to nearly 100 % (Fig. 3A) and accelerated the degradation of PFOA (Fig. 3B and Fig. S6). The degradation rate constant increases from 0.12 (without coexisting constituents) to 0.25 min^{-1} (5 mM chloride) and 0.24 min^{-1} (5 mM sulfate). The presence of humic acid at a high level measured in groundwater slightly slowed the defluorination process and had insignificant effect on the degradation of PFOA (Fig. 3). While 5 mM carbonate slowed the reaction to a larger extent, more than 97 % of degradation and 80 % of defluorination were still achieved after 180 min of treatment.

The promoting effect of chloride and sulfate was contributed by their

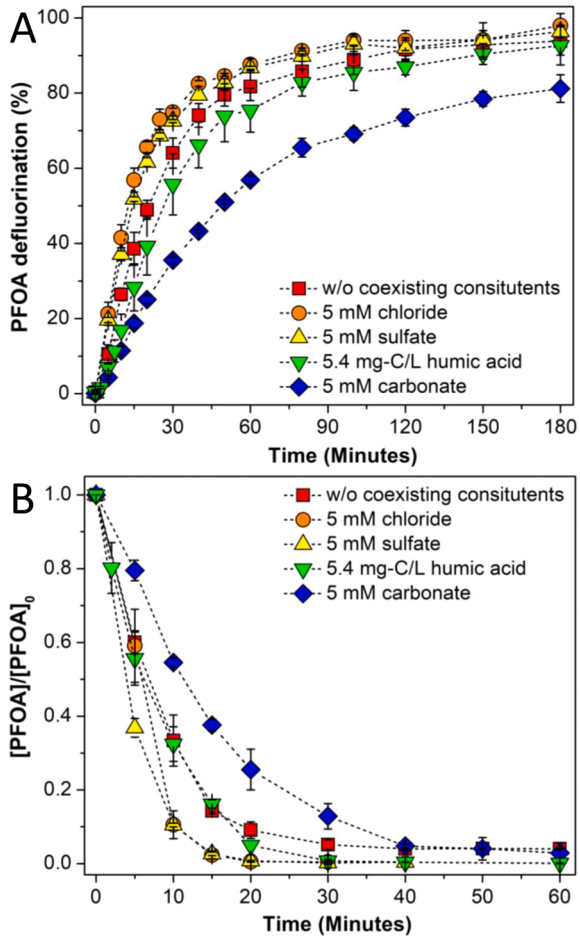

Fig. 3. Impact of coexisting constituents on the destruction of PFOA in H_2-polarized VUV systems. (A) Defluorination of PFOA; (B) Degradation of PFOA. [PFOA] = 25 μM, pH = 12, and [coexisting constituents] = 5 mM or 5.4 mg-C/L. Error bars in panel A represent the differences between duplicate experiments and data points represent the average.

high VUV absorption and high quantum yield of e_{aq}^- in VUV photolysis (Reactions (9) and (10), respectively) (Dainton and Fowles, 1965; Furatian, 2017):

$$Cl^- \xrightarrow{hv} Cl\cdot + e_{aq}^- \quad \varepsilon_{Cl^-,\ 185\ nm} = 3500 M^{-1}\ cm^{-1}\ \Phi_{Cl^-,\ 185nm} = 0.43 \tag{9}$$

$$SO_4^{2-} \xrightarrow{hv} SO_4\cdot - + e_{aq}^- \quad \varepsilon_{SO_4^{2-},\ 185\ nm} = 260\ M^{-1}\ cm^{-1}\ \Phi_{SO_4^{2-},\ 185\ nm} = 0.67 \tag{10}$$

Light partition calculations (Text S2 and Table S4) showed that 5 mM Cl^- absorbed 29 % of VUV light at pH 12.0 and directly photolyzed into e_{aq}^- and Cl· (Reaction (9)). Similarly, 5 mM sulfate absorbed 3 % of VUV light at pH 12.0 and photolyzed into SO_4^- and e_{aq}^- (Reaction (10)). Under alkaline conditions, Cl· and SO_4^- quickly reacted with OH^- to generate hydroxyl radicals. Given that chloride and sulfate generated more reactive species than OH^-, their presence boosted the production of e_{aq}^- in H_2-polarized VUV systems. Calculations (Text S4) showed that $[e_{aq}^-]_{ss}$ increased from 1.4×10^{-12} (without coexisting constituents) to 3.0×10^{-12} M (5 mM chloride) and 2.9×10^{-12} M (5 mM sulfate). Humic acid slightly inhibited the defluorination of PFOA because it reduced the production of e_{aq}^- through screening VUV light and scavenging hydroxyl radical from reacting with H_2. Carbonate slowed the destruction of PFOA to a larger extent because it eliminated the production of e_{aq}^- from the reaction between hydroxyl radicals and H_2. 5 mM carbonate quenched more than 95 % of hydroxyl radicals because carbonate has a higher concentration and faster reaction rate with hydroxyl radicals than with H_2 ($4.0 \times 10^8\ M^{-1}\ s^{-1}$ *vs.* $1.0 \times 10^8\ M^{-1}\ s^{-1}$; 5 mM *vs.* 0.8 mM). The *pseudo* first-order defluorination and degradation rate constants of PFOA was linearly correlated with the production rates of e_{aq}^- under different chemical conditions (Fig. S7), which strongly supported that tuning the production of e_{aq}^- using H_2 is critical to enhance reductive treatment of PFAS in VUV systems.

4. Conclusions

The H_2-polarized VUV water photolysis system provides a promising platform to treat PFAS-contaminated drinking water sources and brine concentrates, because it can directly ionize water molecules and coexisting constituents (*e.g.*, chloride and sulfate) in waste streams to generate e_{aq}^-. The H_2-polarized VUV system quickly destructed PFOA (1300 ng/L) and PFOS (580 ng/L) spiked into a real drinking water matrix, with 95 % degradation achieved within 45-min treatment (Fig. S8). Furthermore, the electrical energy per order (EE/O) for destruction of PFOA under a mild alkaline condition (pH = 10, Fig. S4) is 11 kW h/m^3 (Text S6), which is one order of magnitude lower than that of UVC/sulfite systems at a similar pH (Bentel et al., 2020). Given that only less than 10 % of total photon irradiance from low-pressure mercury lamps was utilized in the VUV system in this study, the energy footprint can be significantly reduced by developing energy-efficient light sources with major photon output at VUV wavelength ranges. We addressed the limitation of VUV light (*e.g.*, short light penetration) in water treatment by minimizing the light attenuation by air, reducing the thickness of the solution surrounding the VUV lamps, and increasing the turbulence of the solution. The performance of the H_2-polarized VUV systems can be further improved by optimizing the lamp type and reactor configurations and enhancing dissolution and diffusion of H_2 gas. More broadly, the H_2-based polarization technique may be readily applied to other water ionization systems to enhance reductive destruction of PFAS and other contaminants. The application of H_2 should performed under proper engineering controls (*e.g.*, ignition source elimination, adequate ventilation, and leak detection). The cost of H_2 can be significantly reduced by recycling and reusing the unutilized H_2 gas out of the solution phase.

Funding Information

the U.S. National Science Foundation Environmental Engineering Program on ERASE-PFAS Initiatives (CBET-2131745).

Declaration of Competing Interest

The authors declare that they have no known competing financial interests or personal relationships that could have appeared to influence the work reported in this paper.

Data Availability

Data will be made available on request.

Acknowledgement

This work was supported by the U.S. National Science Foundation Environmental Engineering Program on ERASE-PFAS Initiatives (CBET-2131745). We thank David Pearson at UCR, and Megan Plumlee and Ken Ishida at Orange County Water District for feedback on the manuscript.

Appendix A. Supporting information

Supplementary data associated with this article can be found in the online version at doi:10.1016/j.hazl.2022.100072.

The Supporting information includes detailed information for experimental setup, figures for degradation and defluorination of PFOS, pseudo-first-order degradation kinetics for PFOA under different experimental conditions, degradation of PFOA and PFOS spiked into in Riverside tap water, and calculation of light partition, branching ratio, and production rates of e_{aq}^- in the H_2-polarized VUV system, volume-normalized photon irradiance to the solution in the reactor, and EE/O.

References

Attri, P., Tochikubo, F., Park, J.H., Choi, E.H., Koga, K., Shiratani, M., 2018. Impact of Gamma rays and DBD plasma treatments on wastewater treatment. Sci. Rep. 8 (1), 1–11.

Barki, D., Sabach, S., Dubowski, Y., 2021. Removal of chlorinated organic pollutants from groundwater using a vacuum-UV-based advanced oxidation process. ACS EST Water 1 (9), 2076–2086.

Bentel, M.J., Yu, Y., Xu, L., Li, Z., Wong, B.M., Men, Y., Liu, J., 2019. Defluorination of per-and polyfluoroalkyl substances (PFASs) with hydrated electrons: structural dependence and implications to PFAS remediation and management. Environ. Sci. Technol. 53 (7), 3718–3728.

Bentel, M.J., Liu, Z., Yu, Y., Gao, J., Men, Y., Liu, J., 2020. Enhanced degradation of perfluorocarboxylic acids (PFCAs) by UV/sulfite treatment: reaction mechanisms and system efficiencies at pH 12. Environ. Sci. Technol. Lett. 7 (5), 351–357.

Biswas, S., Yamijala, S.S., Wong, B.M., 2022. Degradation of per-and polyfluoroalkyl substances with hydrated electrons: a new mechanism from first-principles calculations. Environ. Sci. Technol. 56 (12), 8167–8175.

Boyer, T.H., Fang, Y., Ellis, A., Dietz, R., Choi, Y.J., Schaefer, C.E., Higgins, C.P., Strathmann, T.J., 2021. Anion exchange resin removal of per-and polyfluoroalkyl substances (PFAS) from impacted water: a critical review. Water Res. 200, 117244–117267.

Boyle, J.W., Ghormley, J.A., Hochanadel, C.J., Riley, J.F., 1969. Production of hydrated electrons by flash photolysis of liquid water with light in the first continuum. J. Phys. Chem. 73 (9), 2886–2890.

Bunn, D., Dainton, F., Salmon, G., 1959. The reactivity of hydroxyl radicals in aqueous solution. Part 2.—Relative reactivities with hydrogen, deuterium and hydrogen deuteride. Trans. Faraday Soc. 55, 1760–1767.
Buxton, G.V., Greenstock, C.L., Helman, W.P., Ross, A.B., 1988. Critical review of rate constants for reactions of hydrated electrons, hydrogen atoms and hydroxyl radicals (·OH/·O⁻ in aqueous solution. J. Phys. Chem. Ref. Data 17 (2), 513–886.
Chen, J., Zhang, P., 2006. Photodegradation of perfluorooctanoic acid in water under irradiation of 254 nm and 185 nm light by use of persulfate. Water Sci. Technol. 54 (11–12), 317–325.
Chen, Z., Teng, Y., Mi, N., Jin, X., Yang, D., Wang, C., Wu, B., Ren, H., Zeng, G., Gu, C., 2021. Highly efficient hydrated electron utilization and reductive destruction of perfluoroalkyl substances induced by intermolecular interaction. Environ. Sci. Technol. 55 (6), 3996–4006.
Cui, J., Gao, P., Deng, Y., 2020. Destruction of per-and polyfluoroalkyl substances (PFAS) with advanced reduction processes (ARPs): a critical review. Environ. Sci. Technol. 54 (7), 3752–3766.
Dainton, F.S., Fowles, P., 1965. The photolysis of aqueous systems at 1849 Å II. Solutions containing Cl^-, Br^-, SO_4^{2-} or OH-ions. Proc. R. Soc. Lond. A Math. Phys. Sci. 287 (1410), 312–327.
Dombrowski, P.M., Kakarla, P., Caldicott, W., Chin, Y., Sadeghi, V., Bogdan, D., Barajas-Rodriguez, F., Chiang, S.Y., 2018. Technology review and evaluation of different chemical oxidation conditions on treatability of PFAS. Remediation 28 (2), 135–150.
Duca, C., Imoberdorf, G., Mohseni, M., 2017. Effects of inorganics on the degradation of micropollutants with vacuum UV (VUV) advanced oxidation. J. Environ. Sci. Health A 52 (6), 524–532.
Fang, Y., Ellis, A., Choi, Y.J., Boyer, T.H., Higgins, C.P., Schaefer, C.E., Strathmann, T.J., 2021. Removal of per-and polyfluoroalkyl substances (PFASs) in aqueous film-forming foam (AFFF) using ion-exchange and nonionic resins. Environ. Sci. Technol. 55 (8), 5001–5011.
Fennell, B.D., Mezyk, S.P., McKay, G., 2022. Critical review of UV-advanced reduction processes for the treatment of chemical contaminants in water. ACS Environ. Au 2 (3), 178–205.
Furatian, L., 2017. The use of 185 nm radiation for drinking water treatment. Influence of Temperature and Major Solutes on the Degradation of Trace Organic Contaminants (PhD). The University of British Columbia.
Furatian, L., Mohseni, M., 2018a. Influence of chloride on the 185 nm advanced oxidation process. Chemosphere 199, 263–268.
Furatian, L., Mohseni, M., 2018b. Inuence of major anions on the 185 nm advanced oxidation process-Sulphate, bicarbonate, and chloride. Chemosphere 201, 503–510.
Glüge, J., Scheringer, M., Cousins, I.T., DeWitt, J.C., Goldenman, G., Herzke, D., Lohmann, R., Ng, C.A., Trier, X., Wang, Z., 2020. An overview of the uses of per-and polyfluoroalkyl substances (PFAS). Environ. Sci.: Process. Impacts 22 (12), 2345–2373.
Gonzalez, M.G., Oliveros, E., Wörner, M., Braun, A.M., 2004. Vacuum-ultraviolet photolysis of aqueous reaction systems. J. Photochem. Photobiol. C: Photochem. Rev. 5 (3), 225–246.
Gordon, S., Hart, E.J., Matheson, M.S., Rabani, J., Thomas, J., 1963. Reaction constants of the hydrated electron. J. Am. Chem. Soc. 85 (10), 1375–1377.
Han, P., Bartels, D., 1989. H atom reaction rates in solution measured by free induction decay attenuation. Chem. Phys. Lett. 159 (5–6), 538–542.
Hickel, B., Sehested, K., 1991. Activation energies for the reactions oxide + hydrogen and oxide+ deuterium in aqueous solution. J. Phys. Chem. 95 (2), 744–747.
Hu, X.C., Andrews, D.Q., Lindstrom, A.B., Bruton, T.A., Schaider, L.A., Grandjean, P., Lohmann, R., Carignan, C.C., Blum, A., Balan, S.A., 2016. Detection of poly-and perfluoroalkyl substances (PFASs) in US drinking water linked to industrial sites, military fire training areas, and wastewater treatment plants. Environ. Sci. Technol. Lett. 3 (10), 344–350.
Huang, S., Jaffé, P.R., 2019. Defluorination of perfluorooctanoic acid (PFOA) and perfluorooctane sulfonate (PFOS) by Acidimicrobium sp. strain A6. Environ. Sci. Technol. 53 (19), 11410–11419.
Jin, L., Zhang, P., 2015. Photochemical decomposition of perfluorooctane sulfonate (PFOS) in an anoxic alkaline solution by 185 nm vacuum ultraviolet. Chem. Eng. J. 280, 241–247.
Jing, C., Zhang, P.-y, Jian, L., 2007. Photodegradation of perfluorooctanoic acid by 185 nm vacuum ultraviolet light. J. Environ. Sci. 19 (4), 387–390.
Jortner, J., Ottolenghi, M., Stein, G., 1964. On the photochemistry of aqueous solutions of chloride, bromide, and iodide ions. J. Phys. Chem. 68 (2), 247–255.
Kugler, A., Dong, H., Li, C., Gu, C., Schaefer, C.E., Choi, Y.J., Tran, D., Spraul, M., Higgins, C.P., 2021. Reductive defluorination of perfluorooctanesulfonic acid (PFOS) by hydrated electrons generated upon UV irradiation of 3-Indole-acetic-acid in 12-aminolauric-modified montmorillonite. Water Res. 200, 117221–117229.
Lee, T., Speth, T.F., Nadagouda, M.N., 2021. High-pressure membrane filtration processes for separation of per- and polyfluoroalkyl substances (PFAS). Chem. Eng. J. 134023–134033.
Liu, J., Van Hoomissen, D.J., Liu, T., Maizel, A., Huo, X., Fernández, S.R., Ren, C., Xiao, X., Fang, Y., Schaefer, C.E., 2018. Reductive defluorination of branched per- and polyfluoroalkyl substances with cobalt complex catalysts. Environ. Sci. Technol. Lett. 5 (5), 289–294.
Liu, Y.-L., Sun, M., 2021. Ion exchange removal and resin regeneration to treat per-and polyfluoroalkyl ether acids and other emerging PFAS in drinking water. Water Res. 207, 117781–117790.
Liu, Z., Chen, Z., Gao, J., Yu, Y., Men, Y., Gu, C., Liu, J., 2022. Accelerated degradation of perfluorosulfonates and perfluorocarboxylates by UV/sulfite + iodide: reaction mechanisms and system efficiencies. Environ. Sci. Technol. 56 (6), 3699–3709.
Locke, B., Sato, M., Sunka, P., Hoffmann, M., Chang, J.-S., 2006. Electrohydraulic discharge and nonthermal plasma for water treatment. Ind. Eng. Chem. Res. 45 (3), 882–905.
Lyu, X.-J., Li, W.-W., Lam, P.K., Yu, H.-Q., 2015. Insights into perfluorooctane sulfonate photodegradation in a catalyst-free aqueous solution. Sci. Rep. 5 (1), 1–6.
Masschelein, W.J., Rice, R.G., 2016. Ultraviolet Light in Water and Wastewater Sanitation. CRC press.
Mastropietro, T.F., Bruno, R., Pardo, E., Armentano, D., 2021. Reverse osmosis and nanofiltration membranes for highly efficient PFASs removal: overview, challenges and future perspectives. Dalton Trans. 50 (16), 5398–5410.
McCleaf, P., Englund, S., Östlund, A., Lindegren, K., Wiberg, K., Ahrens, L., 2017. Removal efficiency of multiple poly-and perfluoroalkyl substances (PFASs) in drinking water using granular activated carbon (GAC) and anion exchange (AE) column tests. Water Res. 120, 77–87.
Park, H., Vecitis, C.D., Cheng, J., Choi, W., Mader, B.T., Hoffmann, M.R., 2009. Reductive defluorination of aqueous perfluorinated alkyl surfactants: effects of ionic headgroup and chain length. J. Phys. Chem. A 113 (4), 690–696.
Park, M., Wu, S., Lopez, I.J., Chang, J.Y., Karanfil, T., Snyder, S.A., 2020. Adsorption of perfluoroalkyl substances (PFAS) in groundwater by granular activated carbons: roles of hydrophobicity of PFAS and carbon characteristics. Water Res. 170, 115364–115373.
Patch, D., O'Connor, N., Koch, I., Cresswell, T., Hughes, C., Davies, J.B., Scott, J., O'Carroll, D., Weber, K., 2022. Elucidating degradation mechanisms for a range of per- and polyfluoroalkyl substances (PFAS) via controlled irradiation studies. Sci. Total Environ. 832, 154941–154953.
Ponomarev, A.V., Ershov, B.G., 2020. The green method in water management: electron beam treatment. Environ. Sci. Technol. 54 (9), 5331–5344.
Poskrebyshev, G., Neta, P., Huie, R.E., 2002. Temperature dependence of the acid dissociation constant of the hydroxyl radical. J. Phys. Chem. 106 (47), 11488–11491.
Stoiber, T., Evans, S., Naidenko, O.V., 2020. Disposal of products and materials containing per-and polyfluoroalkyl substances (PFAS): a cyclical problem. Chemosphere 260, 127659–127671.
Sun, Z., Geng, D., Zhang, C., Chen, J., Zhou, X., Zhang, Y., Zhou, Q., Hoffmann, M.R., 2021. Vitamin B12 (CoII) initiates the reductive defluorination of branched perfluorooctane sulfonate (br-PFOS) in the presence of sulfide. Chem. Eng. J. 423, 130149–130157.
United State Environmental Protection Agency: Drinking Water Health Advisories for PFAS Fact Sheet for Communities. ⟨https://www.epa.gov/system/files/documents/2022–06/drinking-water-ha-pfas-factsheet-communities.pdf⟩, (Accessed 6 July 2022).
United State Environmental Protection Agency: Our Current Understanding of the Human Health and Environmental Risks of PFAS. ⟨https://www.epa.gov/pfas/our-current-understanding-human-health-and-environmental-risks-pfas⟩, (Accessed 6 June 2022).
Vecitis, C.D., Park, H., Cheng, J., Mader, B.T., Hoffmann, M.R., 2009. Treatment technologies for aqueous perfluorooctanesulfonate (PFOS) and perfluorooctanoate (PFOA). Front. Environ. Sci. Eng. 3 (2), 129–151.
Wackett, L.P., 2022. Nothing lasts forever: understanding microbial biodegradation of polyfluorinated compounds and perfluorinated alkyl substances. Microb. Biotechnol. 15 (3), 773–792.
Walker, D.C., 1967. The hydrated electron. Q. Rev. Chem. Soc. 21 (1), 79–108.
Wang, J., Lin, Z., He, X., Song, M., Westerhoff, P., Doudrick, K., Hanigan, D., 2022b. Critical review of thermal decomposition of per-and polyfluoroalkyl substances: mechanisms and implications for thermal treatment processes. Environ. Sci. Technol. 56 (9), 5355–5370.
Wang, Y., Zhang, P., 2014. Effects of pH on photochemical decomposition of perfluorooctanoic acid in different atmospheres by 185 nm vacuum ultraviolet. J. Environ. Sci. 26 (11), 2207–2214.
Wang, Y., Longendyke, G., Katel, S., 2022a. PFAS fate and destruction mechanisms during thermal treatment: a comprehensive review. Environ. Sci.: Process. Impacts 24, 196–208.
Wardman, P., 1978. Application of pulse radiolysis methods to study the reactions and structure of biomolecules. Rep. Prog. Phys. 41 (2), 259.
Xiao, X., Ulrich, B.A., Chen, B., Higgins, C.P., 2017. Sorption of poly-and perfluoroalkyl substances (PFASs) relevant to aqueous film-forming foam (AFFF)-impacted groundwater by biochars and activated carbon. Environ. Sci. Technol. 51 (11), 6342–6351.
Xiong, J., Hou, Y., Wang, J., Liu, Z., Qu, Y., Li, Z., Wang, X., 2021. The rejection of perfluoroalkyl substances by nanofiltration and reverse osmosis: influencing factors and combination processes. Environ. Sci.: Water Res. Technol. 7, 1928–1943.
Yamijala, S.S., Shinde, R., Wong, B.M., 2020. Real-time degradation dynamics of hydrated per- and polyfluoroalkyl substances (PFASs) in the presence of excess electrons. Phys. Chem. Chem. Phys. 22 (13), 6804–6808.
Yu, K., Li, X., Chen, L., Fang, J., Chen, H., Li, Q., Chi, N., Ma, J., 2018. Mechanism and efficiency of contaminant reduction by hydrated electron in the sulfite/iodide/UV process. Water Res. 129, 357–364.
Yu, Y., Che, S., Ren, C., Jin, B., Tian, Z., Liu, J., Men, Y., 2022. Microbial defluorination of unsaturated per- and polyfluorinated carboxylic acids under anaerobic and aerobic conditions: a structure specificity study. Environ. Sci. Technol. 56 (8), 4894–4904.
Zhang, Z., Sarkar, D., Biswas, J.K., Datta, R., 2022. Biodegradation of per- and polyfluoroalkyl substances (PFAS): a review. Bioresour. Technol. 344, 126223.
Zoschke, K., Börnick, H., Worch, E., 2014. Vacuum-UV radiation at 185 nm in water treatment–a review. Water Res. 52, 131–145.